J Mater Sci: Mater Electron (2021) 32:15484–15490

Investigation of structural, optical and radiation shielding properties of boron-doped In_2O_3 thin films

Mustafa Kavgacı[1,2,*], Adnan Küçükönder[1], and Süleyman Kerli[3]

[1] *Department of Physics, Kahramanmaras Sutcu Imam University, Kahramanmaraş, Turkey*
[2] *Department of Opticianry, Elbistan Vocational School of Health Services, Kahramanmaraş Istiklal University, Kahramanmaraş, Turkey*
[3] *Department of Energy Systems Engineering, İstiklal University, Kahramanmaraş, Turkey*

Received: 25 February 2021
Accepted: 30 April 2021
Published online: 24 May 2021

© The Author(s), under exclusive licence to Springer Science+Business Media, LLC, part of Springer Nature 2021

ABSTRACT

Indium oxide and boron-doped indium oxide thin films were produced using the spray pyrolysis method. XRD measurements were made to determine the structural properties of these synthesized films, and it was observed that the films had a cubic structure. Morphological properties were examined, and it was observed that films were generally homogeneous. It has been observed from the Uv–Vis spectrometer measurements that the transmittance rates increase with the boron doping. The mass and linear attenuation coefficients, half-value layer, mean free path and tenth value layer of different percentages for undoped and boron-doped thin films were investigated experimentally. Electron detector and 6 MeV energy electrons were used in irradiation to make these measurements. The experimental results determined that added boron to indium oxide thin films positively contributed to the radiation shielding property.

1 Introduction

Developments in radiation technology cause us to be more exposed to different radiation sources day by day. Due to rapid technological advances, many types of radiation are exposed from different sources such as X-rays, medical instruments and factory waste. Developing of radiation sources and their applications in various fields leads to an increase importance of radiation shielding. Many studies have been conducted on the radiation protection properties of concrete, alloys, rocks, natural and glass materials [1–5]. Many studies have reported that glass materials have considerable radiation shielding ability [6]. For example, radiation shielding properties were investigated by coating metal oxide thin film on glasses [7].

Various methods exist to produce thin films [8–14]. Spray pyrolysis method, one of these methods, is efficient, easy to apply and cost-effective [15, 16]. This method allows high-quality production [17]. Large areas can be covered by the spray pyrolysis method. [18]. It is a method suitable for fast and industrial production [19].

Address correspondence to E-mail: mkavgaci@gmail.com

https://doi.org/10.1007/s10854-021-06097-w

Thin films produced with different metal oxides have attracted the attention of many studies [20–25]. Among these metal oxides, indium oxide thin films are notable for their physical properties such as good electrical conductivity, chemical stability, hardness, high permeability in visible and infrared regions [26]. Indium oxide thin films have an important place in the industry due to its various application areas such as optoelectronic devices, solar cells, transistors, gas sensors, liquid crystal displays, diodes, dosimeters, sensors, electron radiation fields, photocatalysis, thermoelectric [26–31]. However, the research examining the effect of radiation on indium oxide thin films is insufficient in the literature [32].

In this study, boron-doped indium oxide thin films were produced by the spray pyrolysis method. Radiation permeability properties of thin films were investigated. This study's primary purpose is to investigate the radiation absorption properties of indium oxide thin films doped with boron at different percentages.

2 Materials and methods

2.1 Synthesis of boron-doped indium oxide films

The solution was prepared using ultrapure water and 50 mL of 0.1 M $InCl_3$ (indium (III) chloride 98%, Sigma-Aldrich). Boron (H_3BO_3, Sigma-Aldrich) was doped in the solutions with atomic percentage 0, 5, 10 and 20% relative to indium. They will be named as 0% boron-doped films InO, 5% boron-doped films In5B, 10% boron-doped films In10B and 20% boron-doped films In20B. Substrates were cleaned with ethyl alcohol (Alfa-Aesar) and distilled water, then dried. Thin films are covered with a homemade spray pyrolysis system of our own design. During the coating, the temperature of the substrates was set to 450 °C. The synthesized films were then annealed at 550 ° C for 2 h.

2.2 Characterization

The diffraction pattern of thin films was determined using a Philips X'Pert PRO brand XRD with CuKα radiation (λ = 0.154056 nm, set at 40 kV-30 mA) device. Morphological properties of the films were observed in the ZEISS EVO LS10 with 10 kV scanning electron microscope. Shimadzu 1800 spectrometer was used to examine its optical properties.

2.2.1 Theoretical basis

The probability of radiation to interact with a given material per unit length is defined as the linear attenuation coefficient (μ)(LAC) [33]. LAC is a parameter that defines the resistance of the material to incoming radiation [1].

$$\mu\left(\mathrm{cm}^{-1}\right) = \frac{1}{\times}\ln\left(\frac{I}{I_0}\right) \tag{1}$$

In Eq. (1), x is the thickness of thin films, I is the number of electrons in the presence of thin films, and I_0 is the number of electrons in the absence of thin film. Equation (2) is the standard deviation of the linear attenuation coefficients [7].

$$\sigma = \sqrt{\frac{\sum_{i=1}^{N}\left(\mu_i - \bar{\mu}\right)^2}{N-1}} \tag{2}$$

where μ_i is the linear attenuation coefficients of thin films and $\bar{\mu}$ is the average linear attenuation coefficient of thin films and N is the number of counts per sample [7].

The mass attenuation coefficient(MAC) of a mixture or compound is calculated by Eq. (3) [34].

$$\mu_m\left(\frac{\mathrm{cm}^2}{g}\right) = \sum_{i=0}^{n}\omega_i\left(\frac{\mu}{\rho}\right)_i \tag{3}$$

where ω_i is the weight fraction and $\left(\frac{\mu}{\rho}\right)_i$ is MAC for each element in the compound [34].

Fraction by weight for a chemical compound [35] is,

$$\omega_i = \frac{n_i A_i}{\Sigma_j n_j A_j} \tag{4}$$

In the equation, A_i is atomic weight of the element in the compound and n_i is the number of atoms of the element [36].

The half value layer(HVL) is the thickness of the material that passes half the radiation interacting with the material [37]:

$$\mathrm{HVL} = \frac{\ln 2}{\mu} \tag{5}$$

The required shield thickness reduces the transmitted radiation to one tenth of the initial intensity (TVL) [38]:

$$\mathrm{TVL} = \frac{\ln 10}{\mu} \tag{6}$$

Mean free path(MFP) between the successive interactions of an electron with the material [7]:

$$\mathrm{MFP} = \frac{1}{\mu} \tag{6}$$

is found with equations [39].

2.2.2 *Experimental setup*

The irradiation of thin films was done using a VARIAN® linear accelerator [7]. Thin films were exposed to electrons with 6 MeV energy after being placed between solid phantoms. Due to the 6 MeV electrons' Dmax, a 13 mm solid phantom was used for the measurements. Dose measurements were taken using a PTW® electron detector [7] and a 6 × 6 cm electron field applicator [40]. The source was set 100 cm from the thin films. Detector was placed under thin films [5]. The experimental setup is shown in Fig. 1.

3 Results and discussion

Structural analysis of pure and boron-doped indium oxide thin films was performed using the X-ray diffraction (XRD) method. Figure 2 shows the XRD graph of indium oxide (In_2O_3) and boron-doped indium oxide thin films. XRD results are suitable with reference PDF-2 00-006-0416. In the diffraction pattern, the peaks corresponding to the planes (211), (222), (400), (440) and (622) are quite visible. The peaks agree with the studies in the literature and show that thin films have a cubic structure. [41]. No peak of the boron element or its compounds doped to thin films was found. In_2O_3 thin films have some defects such as indium and oxygen voids. The occupation of the intermediate areas by the doping atoms creates deterioration in the crystal structure [42]. It is seen that the density of the peak (400) in the diffraction pattern after doping is significantly reduced. As the amount of boron doping increases from the XRD graph, decreases in the peak intensity are observed. The reason for this can be explained by the deterioration of the indium oxide structure by the inclusion of boron in the interstitial regions [43, 44].

SEM images showing the surface morphology of the synthesized indium oxide and boron-doped indium oxide thin films are given in Fig. 3. SEM images showed that the thin films produced hold on well to the surface. It has been observed to be generally homogeneous.

The measured transmission and absorption of thin films are given in Fig. 4. It appears that boron-doped indium oxide films have low absorption between 400 and 700 nm wavelengths (Fig. 4a). The reason for this may be due to its low surface roughness and better homogeneity [45]. As seen in Fig. 4b, indium oxide thin films have a transmittance rate of approximately 59% at 900 nm wavelength. Also, it was determined that the transmittance of the thin films increased as the amount of boron increased. In general, In20B thin film has the highest transmittance value.

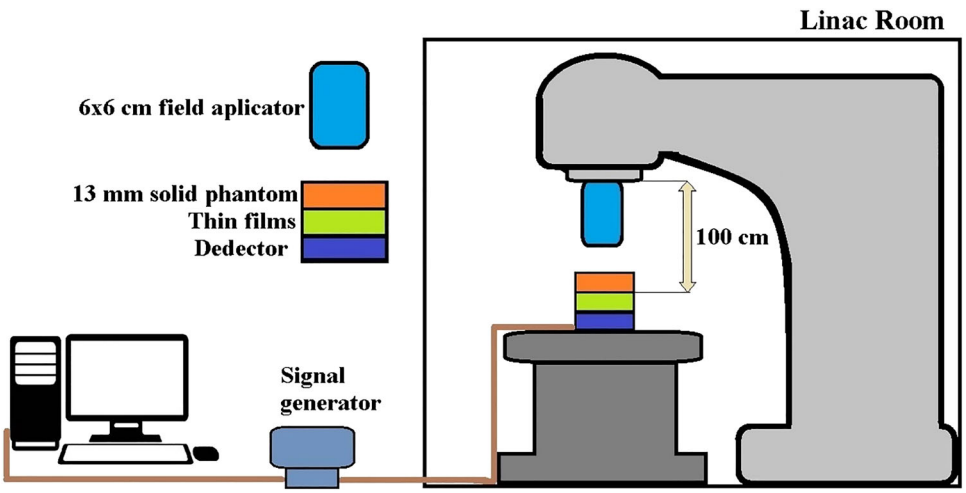

Fig. 1 Scheme of the experimental setup (decorated inspired by [7])

LAC is an important indicator for the radiation protection efficiency of thin films. All thin films were irradiated with 6 MeV electrons. The results of LAC (μ), MAC (μm), HVL, TVL and MFP of all thin films are given in Table 1. As can be seen from the values given in Table 1, the boron contribution has positively affected all values. The highest value of LAC was obtained for In20B thin film (0.0051 ± 0.0008 cm^{-1}) and the lowest value has been found In5B thin film (0.0038 ± 0.00009 cm^{-1}). LAC values are shown in Fig. 5.

MAC of all thin films is shown in Fig. 6. As the boron dope amount increases, MAC increases. The highest MAC value belongs to 20% boron-doped indium oxide thin film (0.00101 ± 0.00024cm^2).

MFP, HVL and TVL values of thin films are given in Fig. 7. MFP, HVL and TVL values decrease with the increase in the amount of boron-doped in In_2O_3 thin films. According to the amount of boron-doped in indium oxide thin films, the half value layer decreased from 327.69 to 133.77 cm, the tenth layer value decreased from 1088.56 to 444.37 cm, the mean free path value decreased from 472.76 to 192.98 cm.

In addition to this work, research can be done for different types of radiation and particles. Interactions with different radiation sources can be studied [29, 46–48]. In addition, more information can be obtained with new researches on the structural, morphological, optical and radiation permeability properties of these thin films [49].

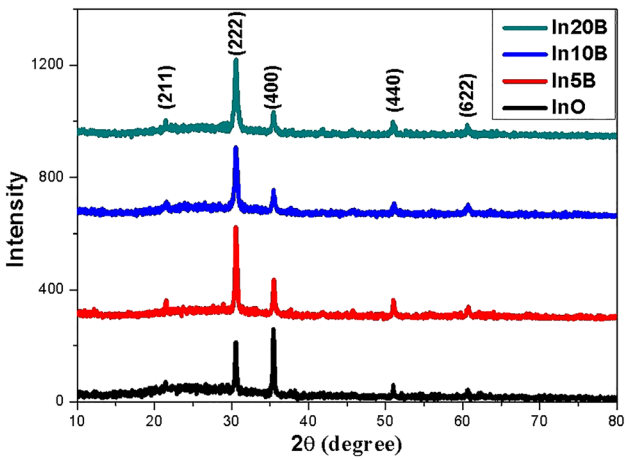

Fig. 2 XRD pattern of In_2O_3 and boron-doped In_2O_3 thin films

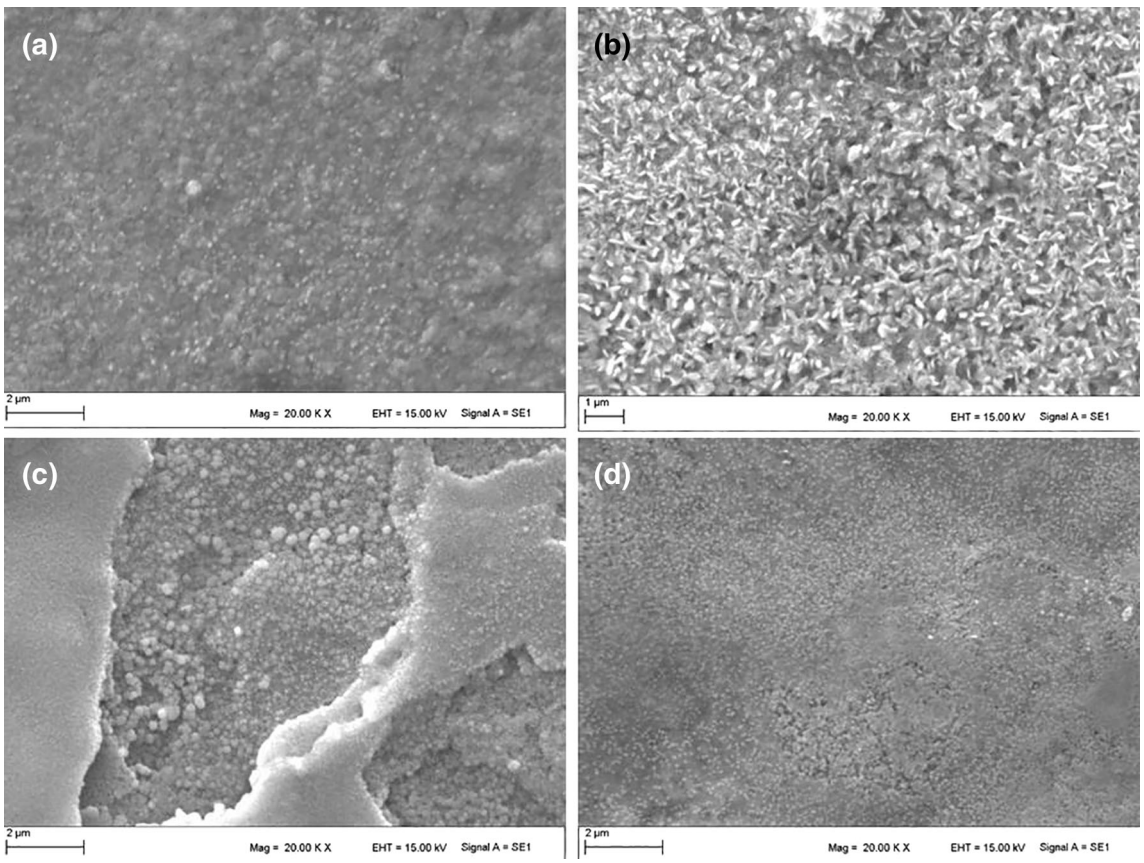

Fig. 3 SEM images **a** InO **b** In5B **c** In10B **d** In20B

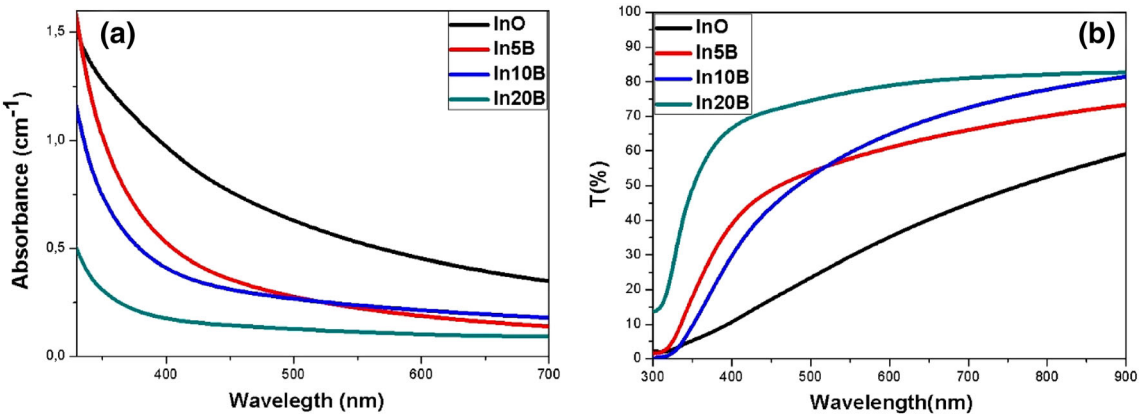

Fig. 4 **a** Absorbance spectrum of In_2O_3 and boron-doped In_2O_3 thin films **b** Transmittance spectrum of In_2O_3 and boron-doped In_2O_3 thin films

Table 1 LAC, MAC, HVL, TVL and MFP values of In_2O_3 and boron-doped In_2O_3 thin films

Compositions (%)		LAC (cm^{-1})	MAC (cm^2/g)	MFP (cm)	HVL (cm)	TVL (cm)
In_2O_3	B					
100	0	0.0021 ± 0.0013	0.00029 ± 0.00026	472.76	327.69	1088.56
95	5	0.0038 ± 0.00009	0.00059 ± 0.00005	260.85	180.81	600.63
90	10	0.0047 ± 0.0005	0.00079 ± 0.00008	211.75	146.77	487.57
80	20	0.0051 ± 0.0008	0.00101 ± 0.00024	192.98	133.77	444.37

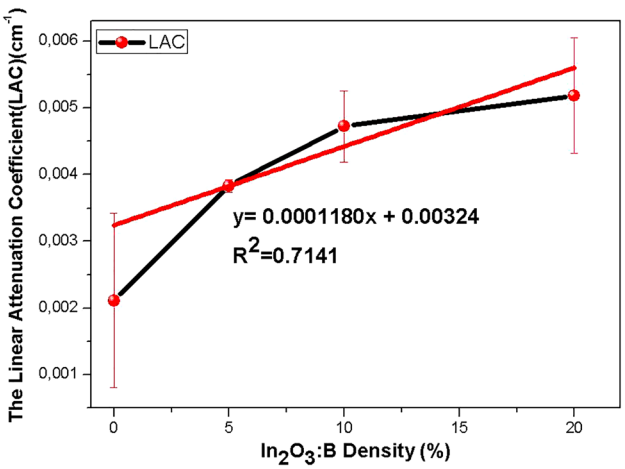

Fig. 5 LAC of InO, In5B, In10B and In20B thin films

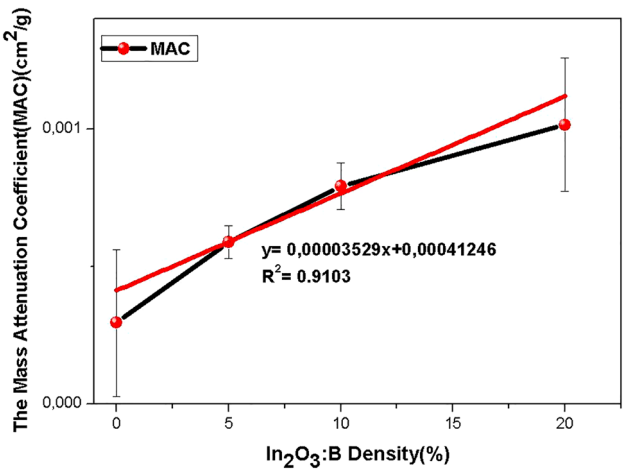

Fig. 6 MAC of InO, In5B, In10B and In20B thin films

4 Conclusions

Structural, morphological, optical and radiation shielding properties produced with spray pyrolysis method pure and boron-doped In_2O_3 thin films were investigated. XRD analysis showed that the prepared films had a cubic structure. It was observed from the SEM images that the films were homogeneous in morphology. Radiation shielding properties of thin films irradiated with electrons were investigated. It has been determined that boron doping has a positive contribution to the radiation shielding parameters. As the amount of boron-doped in In_2O_3 thin films increased, the linear and mass attenuation coefficient also increased. The half-value layer, one-tenth value layer values and the mean free path also decreased with the increase in the amount of boron additives in thin films. These results showed that indium oxide

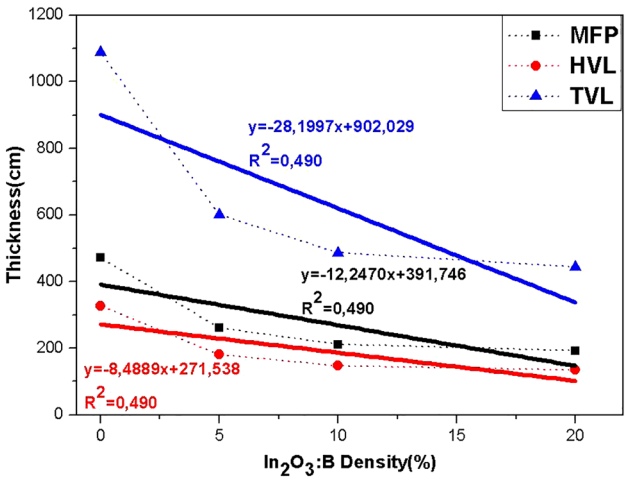

Fig. 7 MFP, HVL and TVL values of InO, In5B, In10B and In20B thin films

can be used as a radiation shield by doping boron in thin films.

Acknowledgements

This study was supported by the Scientific Research Projects Coordination Unit of Kahramanmaras Sutcu Imam University. Project Number 2020/9–23 D.

References

1. A. Mansour, M.I. Sayyed, K.A. Mahmoud, E. Şakar, E.G. Kovaleva, J. Radiat. Res. Appl. Sci. **13**, 94 (2020)
2. B. Mavi, Ann. Nucl. Energy **44**, 22 (2012)
3. S.S. Obaid, M.I. Sayyed, D.K. Gaikwad, P.P. Pawar, Radiat. Phys. Chem. **148**, 86 (2018)
4. Y. Kavun, İ Boztosun, H. Đapo, İ Maraş, C. Segebade, Radiochim. Acta **106**, 759 (2018)
5. Y. Kavun, A. Tutus, S. Uruş, A. Tutuş, S. Eken, R. Özbek, Cumhur. Sci. J. CSJ E **40**, 846 (2019)
6. S.A.M. Issa, H.O. Tekin, R. Elsaman, O. Kilicoglu, Y.B. Saddeek, M.I. Sayyed, Mater. Chem. Phys. **223**, 209 (2019)
7. H. Eskalen, Y. Kavun, S. Kerli, S. Eken, Opt. Mater. (Amst). **105**, 109871 (2020)
8. U. Alver, H. Yaykaşlı, S. Kerli, A. Tanrıverdi, Int. J. Miner. Metall. Mater. **20**, 1097 (2013)
9. S. Benramache, Y. Aoun, Ann. West Univ. Timisoara Phys. **61**, 56 (2020)
10. K. Daoudi, B. Canut, M.G. Blanchin, C.S. Sandu, V.S. Teodorescu, J.A. Roger, Thin Solid Films **445**, 20 (2003)
11. L.G. Bloor, J. Manzi, R. Binions, I.P. Parkin, D. Pugh, A. Afonja, C.S. Blackman, S. Sathasivam, C.J. Carmalt, Chem. Mater. **24**, 2864 (2012)
12. S.Y. Lee, B.O. Park, Thin Solid Films **484**, 184 (2005)
13. B.G. Durdu, U. Alver, A. Kucukonder, Ö. Sögüt, M. Kavgaci, Acta Phys. Pol. A **124**, 41 (2013)
14. U. Alver, T. Kilinç, E. Bacaksiz, S. Nezir, Mater. Chem. Phys. **106**, 227 (2007)
15. A.S. AlShammari, M.M. Halim, F.K. Yam, N.H.M. Kaus, Mater. Sci. Semicond. Process. **116**, 105140 (2020)
16. R. Thomas, T. Mathavan, M.A. Jothirajan, H.H. Somaily, H.Y. Zahran, I.S. Yahia, Opt. Mater. (Amst) **99**, 109518 (2020)
17. D. Selleswari, P. Meena, D. Mangalaraj, J. Iran. Chem. Soc. **16**, 1291 (2019)
18. R. Gandasiri, C.J. Sreelatha, P. Nagaraju, Y. Vijayakumar, Phys. B Condens. Matter **572**, 220 (2019)
19. S. Palanichamy, J.R. Mohamed, K.D.A. Kumar, S.K. Satheesh, S. Pandiarajan, L. Amalraj, Optik (Stuttg) **194**, 162887 (2019)
20. F. Chandoul, A. Boukhachem, F. Hosni, H. Moussa, M.S. Fayache, M. Amlouk, R. Schneider, Ceram. Int. **44**, 12483 (2018)
21. S. Kerli, Ü. Alver, H. Eskalen, S. Uruş, A.K. Soğuksu, Russ. J. Appl. Chem. **92**, 304 (2019)
22. P. Dong, B. Yang, C. Liu, F. Xu, X. Xi, G. Hou, R. Shao, RSC Adv. **7**, 947 (2017)
23. M. Aftab, M.Z. Butt, D. Ali, F. Bashir, Z.H. Aftab, Ceram. Int. **46**, 5037 (2020)
24. B. Bozkurt Çırak, Ç. Eden, Y. Erdoğan, Z. Demir, K.V. Özdokur, B. Caglar, S. Morkoç Karadeniz, T. Kılınç, A. Ercan Ekinci, Ç. Çırak, Optik (Stuttg) **203**, 163963 (2020)
25. J. Morales, L. Sánchez, F. Martín, J.R. Ramos-Barrado, M. Sánchez, Thin Solid Films **474**, 133 (2005)
26. C. Nefzi, M. Souli, N. Beji, A. Mejri, N. Kamoun-Turki, J. Mater. Sci. **52**, 336 (2017)
27. A. Qurashi, E.M. El-Maghraby, T. Yamazaki, Y. Shen, T. Kikuta, J. Alloys Compd. **481**, L35 (2009)
28. A. Sudha, T.K. Maity, S.L. Sharma, Mater. Lett. **164**, 372 (2016)
29. C. Nefzi, N. Beji, M. Souli, A. Mejri, S. Alleg, N. Kamoun-Turki, Opt. Laser Technol. **112**, 85 (2019)
30. L.G. Bloor, C.J. Carmalt, D. Pugh, Coord. Chem. Rev. **255**, 1293 (2011)
31. P.P. Murmu, A. Shettigar, S.V. Chong, Z. Liu, D. Goodacre, V. Jovic, T. Mori, K.E. Smith, J. Kennedy, J. Mater. **7**, 612 (2021)
32. A. Sudha, S.L. Sharma, A.N. Gupta, Sens. Actuators A Phys. **285**, 378 (2019)

33. B. Alım, E. Şakar, A. Baltakesmez, İ Han, M.I. Sayyed, L. Demir, Radiat. Phys. Chem. **166**, 108455 (2020)
34. Z.I. Takai, R.S. Kaundal, M.K. Mustafa, S. Asman, A. Idris, Y. Shehu, J. Mohammad, M.G. Idris, M. Said, Mater. Res. **22**, 20180404 (2018)
35. A. Levet, E. Kavaz, Y. Özdemir, J. Alloys Compd. **819**, 152946 (2020)
36. F. Akman, R. Durak, M.F. Turhan, M.R. Kaçal, Appl. Radiat. Isot. **101**, 107 (2015)
37. M. Wilson, Mater. Chem. Phys. **224**, 238 (2019)
38. B. Oto, E. Kavaz, H. Durak, A. Aras, Z. Madak, Ceram. Int. **45**, 23681 (2019)
39. D. Yılmaz, B. Aktaş, A. Çalık, O.B. Aytar, Radiat. Phys. Chem. **161**, 55 (2019)
40. S. Chen, S. Nambiar, Z. Li, E. Osei, J. Darko, W. Zheng, Z. Sun, P. Liu, J.T.W. Yeow, J. Mater. Sci. **54**, 3023 (2019)
41. H.-C. Pan, M.-H. Shiao, C.-Y. Su, C.-N. Hsiao, J. Vac. Sci. Technol. A Vac. Surf. Film **23**, 1187 (2005)
42. N. Beji, M. Souli, S. Azzaza, S. Alleg, N. Kamoun Turki, J. Mater. Sci. Mater. Electron. **27**, 4849 (2016)
43. S. Arulkumar, S. Parthiban, D. Gnanaprakash, J.Y. Kwon, J. Mater. Sci. Mater. Electron. **30**, 18696 (2019)
44. K.A. Stewart, V. Goulioukk, D.A. Keszler, J.F. Wager, Solid State Electron. **137**, 80 (2017)
45. Z.N. Kayani, Z. Bashir, S. Riaz, S. Naseem, Z. Saddiqe, J. Mater. Sci. Mater. Electron. **31**, 11911 (2020)
46. Y. Zhao, R. Ning, X. Yi, Z. Gao, H. Wang, W. Cai, Mater. Charact. **164**, 110348 (2020)
47. M. Maaza, O. Nemraoui, A.C. Beye, C. Sella, T. Derry, Sol. Energy Mater. Sol. Cells **90**, 111 (2006)
48. F. Cataldo, M. Prata, J. Radioanal. Nucl. Chem. **320**, 831 (2019)
49. D. Yılmaz, Z. Uzunoğlu, A. Baltakesmez, F. Özçelik, B. Güzeldir, Radiat. Phys. Chem. **166**, 108460 (2020)

Publisher's Note Springer Nature remains neutral with regard to jurisdictional claims in published maps and institutional affiliations.